JMEPEG (2004) 13:758-765
DOI: 10.1361/10599490420566

1059-9495/$19.00

Effect of Notch Location on Fatigue Crack Growth Behavior of Strength-Mismatched High-Strength Low-Alloy Steel Weldments

S. Ravi, V. Balasubramanian, and S. Nemat Nasser

(Submitted July 8, 2003)

Welding of high-strength low-alloy (HSLA) steels involves the use of low-strength, equal-strength, and high-strength filler materials (electrodes) compared with the parent material, depending on the application of the welded structures and the availability of filler material. In the present investigation, the fatigue crack growth behavior of weld metal (WM) and the heat-affected zone (HAZ) of undermatched (UM), equally matched (EM), and overmatched (OM) joints has been studied. The base material used in this investigation is HSLA-80 steel of weldable grade. Shielded metal arc welding (SMAW) has been used to fabricate the butt joints. A center-cracked tension (CCT) specimen has been used to evaluate the fatigue crack growth behavior of welded joints, utilizing a servo-hydraulic-controlled fatigue-testing machine at constant amplitude loading (R = 0). The effect of notch location on the fatigue crack growth behavior of strength mismatched HSLA steel weldments also has been analyzed.

Keywords fatigue crack growth, fatigue life, high-strength low-alloy steel, mismatch ratio, notch location, shielded metal arc welding

1. Introduction

Welded structures have been used in the power-generation, offshore structure building, transportation, and aerospace industries. Welded joints are sensitive areas of the structural system because they are complex metallurgically and exhibit complicated stress conditions. The yield strength/tensile strength ratio of the weld metals (WMs) that were used for welding the mild steel in early designs was very high, and the designers did not pay much attention to the yield strength of the WMs (Ref 1). With the increased use of high-strength alloys, it is very difficult to produce the matching and overmatching welding consumables, because the strength and toughness cannot be increased simultaneously. Sometimes, the yield strength of the WM used for joining the plates is lower (undermatched [UM]) or higher (overmatched [OM]) than the yield strength of the base alloy filler material (Ref 2).

Mismatched welded joints are joints in which the yield strength and/or the microstructures of the WM will be different from that of the base metal and the heat-affected zone (HAZ). The factors that are responsible for heterogeneities include the welding process, welding consumables, joint design, and weld thermal cycles. UM joints are used in repair welding, and in the welding of penstock, pressure vessels, and bridges, for example. They are used to prevent the formation of cracks in the welds; for example, a UM cap pass reduces the weld toe cracking from cyclic plastic bending during reeling (Ref 3). Similarly, OM joints are used in pipeline girth welds, welded offshore structures, and cladding and hard facing, and for protecting the WM failure by effectively shielding the small cracks present in the WM (Ref 4).

In the base metal, HAZ and WM combinations, both global mismatch and local mismatch, cause the mismatch constraint. The global mismatch is defined as the ratio of the yield strength of WM to that of the base metal, whereas the local mismatch is defined as the ratio of the yield strength of the WM to that of the HAZ. The mechanical factors responsible for producing the global strength mismatch in the weldment are base metal yield strength, WM yield strength, base metal tensile strength, and WM tensile strength. The net section yielding occurs when plastic deformation is confined to the defective cross section. Gross section yielding occurs when the applied stress exceeds the alloy yield strength, i.e., when the yield strength of the WM exceeds that of the base metal. In general, large defects tend to produce net section yielding, whereas small defects are beneficial for obtaining gross section yielding (Ref 5).

Recently, some studies (Ref 6, 7) have been conducted to assess the fracture behavior of mismatched weldments and bimaterial joints by varying the mismatch ratio (MMR) (the ratio between the yield strength of WM and the yield strength of the base metal). It has been found that little engineering experience (Ref 8, 9) on the performance of high-strength steel joints has been gained, especially concerning strength-mismatched joints under cyclic loading conditions. Hence, the main objective of the present investigation was to study and analyze the effect of notch location on fatigue crack growth behavior and fatigue life on shielded metal arc welded, strength-mismatched, high-strength low-alloy (HSLA) steel weldments.

2. Experimental

The base alloy used in this investigation was HSLA-80 steel, which is widely used for such items as submarines,

S. Ravi and **V. Balasubramanian,** Department of Manufacturing Engineering, Annamalai University, Annamalainagar 608 002, Tamil Nadu, India; and **S. Nemat Nasser,** Centre of Excellence for Advanced Materials, University of California at San Diego, La Jolla, CA 92093-0416. Contact e-mail: visvabalu@yahoo.com.

bridges, heavy earth moving equipment, pressure vessels, pipelines, ships, and offshore structures (Ref 10). Rolled plates, 12 mm thick, have been used as the base alloy in the welding studies. A single-bevel butt joint, as shown in Fig. 1, has been prepared for joining the plates. This joint design was chosen to study the fatigue crack growth behavior in the HAZ region, since this joint is straight and parallel. Three types of low-hydrogen, ferritic electrodes with different yield strengths have been chosen for joining the plates to attain the desired strength MMRs. The chemical composition of the base alloy and WMs are presented in Table 1, and their mechanical properties are presented in Table 2. The welding conditions and weld process parameters used in the fabrication of the joints are given in Table 3.

The welded joints were sliced and then machined to the required dimensions (as shown in Fig. 2) for center-cracked tension (CCT) fatigue crack growth test specimens. The notch was machined (in both the WM and HAZ regions) using wire electric-discharge machining (EDM). Fatigue crack growth experiments were conducted using a servo hydraulic, 100 kN universal testing machine. A frequency of 20 Hz under constant amplitude loading ($R = 0$) was used for all fatigue tests. Before loading, the specimen surface near the notch was polished to facilitate fatigue crack growth measurement. A traveling microscope with an accuracy of 0.01 mm was used to monitor the crack length. The specimen was loaded at a particular stress level (range), and following crack initiation from the tip of the machined notch, its subsequent propagation into the WM and HAZ, respectively, was recorded from initiation to the complete failure of the specimen. Similar crack growth experiments were conducted on a number of specimens at various stress levels, and the experimental data were recorded.

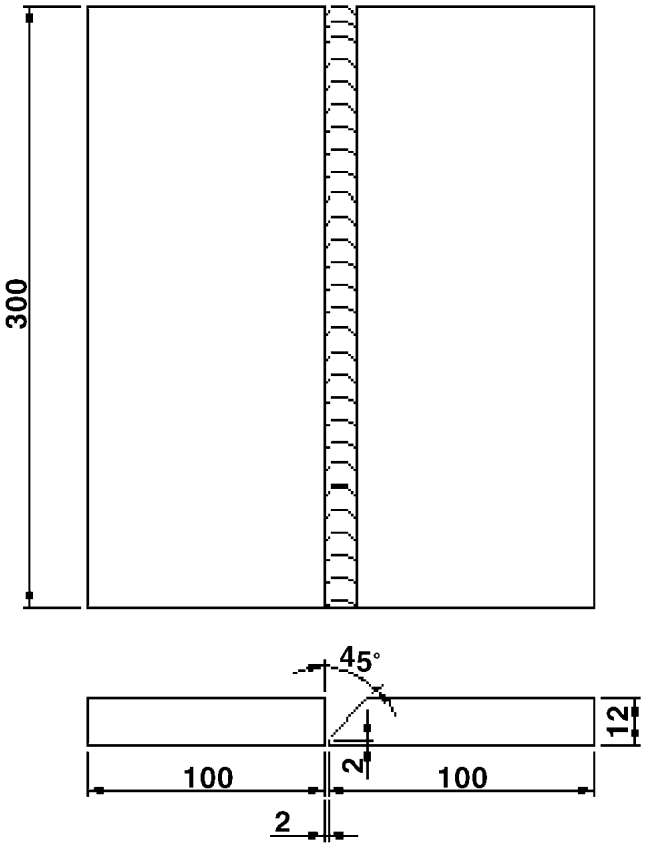

Fig. 1 Joint configuration

3. Results

The fatigue crack growth experiments were conducted at 75, 100, 125, and 150 MPa and under constant amplitude loading conditions. The variation in crack length ($2a$) with number of cycles (N) was recorded. The Paris equation (Ref 11) was used to analyze the experimental results.

$$da/dN = C\,(\Delta K)^m \quad \text{(Eq 1)}$$

where da/dN is the crack growth rate, ΔK is the stress intensity factor (SIF) range, and C and m are constants. The SIF value was calculated for different values of the growing fatigue crack using the following expression (Ref 12):

$$\Delta K = \phi\,(\Delta\sigma)\,\sqrt{\pi\, a} \quad \text{(Eq 2)}$$

However, the geometry factor ϕ for the CCT specimen was calculated using the expression given below (Ref 13):

$$\phi = F(\alpha) = \sec\left\{\frac{(\alpha)}{2}\right\} \quad \text{(Eq 3)}$$

In Eq 3, α is equal to (a/W) and pi is a function of α and is defined by F.

The crack growth rate, $d(2a)/dN$ for the propagation stage, was calculated for the steady-state growth regimen at different intervals of the crack length increment. The relationship between SIF range and the corresponding crack growth rate in terms of "best-fit" line is shown in Fig. 3 for both the WM and HAZ. The data correspond to the second stage of the Paris sigmoidal relationship, i.e., from 10^{-6} to 10^{-3} mm/cycle. The exponent m (i.e., the slope of the line on a log-log plot) and C have been determined and are presented in Table 4. In the present analysis, the relation obtained is a sigmoidal type, with

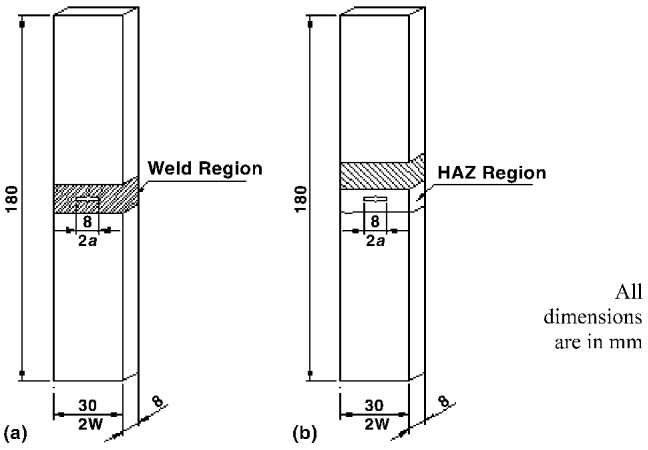

Fig. 2 Dimensions of the CCT specimen

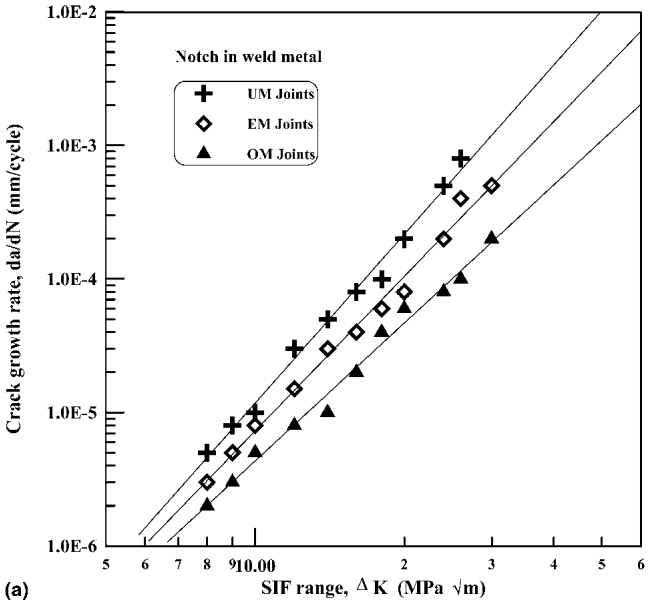

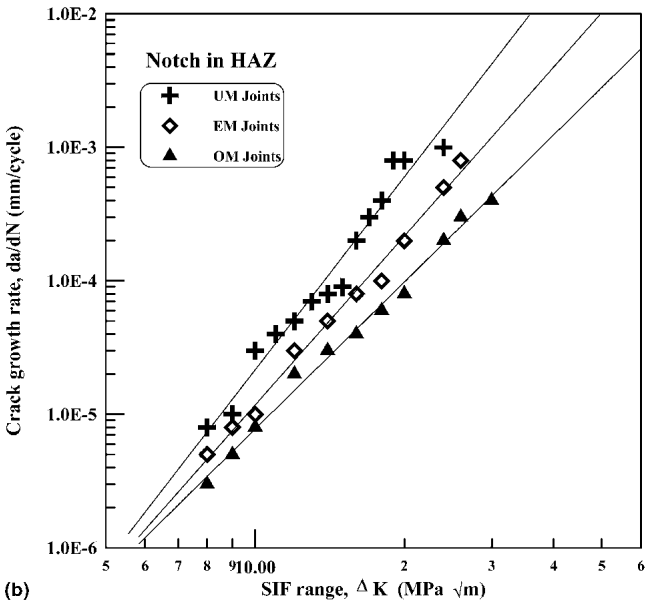

Fig. 3 Crack growth rate curves

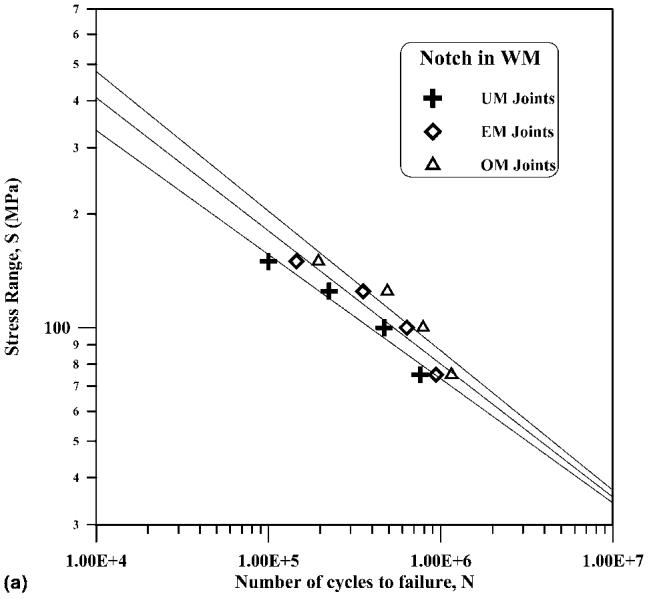

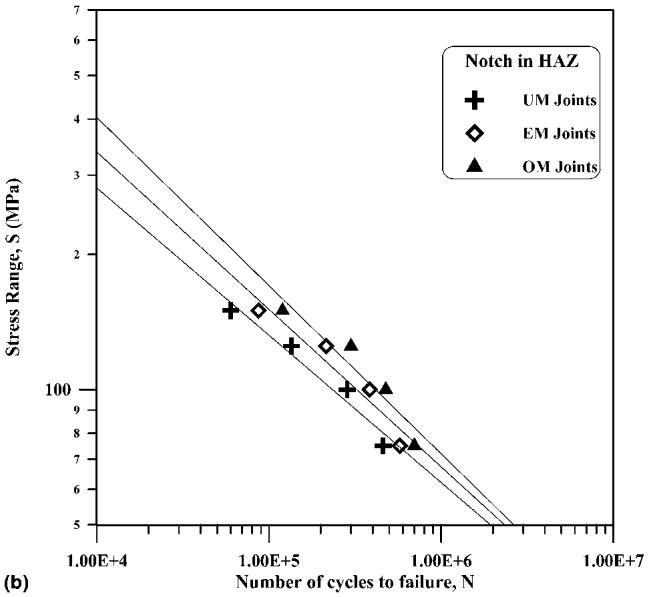

Fig. 4 *S-N* curves

the curve tending to become parallel to the Y-axis (*da*/*dN*) when the SIF is low or very high. However, at high values of ΔK, the exponent increases. When the crack growth rate is around 10^{-3} mm/cycle, the curve tends to become parallel to the Y-axis, and the corresponding ΔK value is taken as critical (ΔK_{cr}).

At lower values of ΔK, the curve again becomes parallel to the Y-axis, indicating a threshold SIF (ΔK_{th}) below which a crack may not propagate. The values of ΔK_{cr} and ΔK_{th} for all joints have been evaluated and are presented in Table 4. Normally, in the case of steels, the threshold value is obtained for a crack growth rate of 10^{-8} mm/cycle. Due to the specimen configuration and loading conditions, crack propagation rates in the region of 10^{-8} mm/cycle could not be obtained, and hence the value obtained in this analysis cannot be taken as the design value. The fatigue crack growth (fracture mechanics) parameters of all the joints are compared in Table 4.

It is also advantageous to determine the standard *S-N* curve for the test conditions, which will indicate the trend and also be useful for design purposes. Figure 4 shows the relationship between stress range and the number of cycles to failure on a log-log plot for all the joints. The stress corresponding to 2×10^6 cycles is taken as an indication of the endurance limit (Ref 14), and these values are determined for all the joint combinations and are presented in Table 4.

4. Discussion

From the crack growth rate curves (Fig. 3), it is evident that the resistance offered by the OM WM and OM HAZ is higher

Table 1 Chemical composition of base metal and WMs

	Composition, wt. %										
Element	**C**	**Si**	**Mn**	**P**	**S**	**Cr**	**Mo**	**Ni**	**Cu**	**V**	**Fe**
BM	0.06	0.40	0.70	0.02	0.01	0.80	0.25	1.0	0.90	0.05	Bal
UM WM	0.08	0.66	1.27	0.02	0.03	…	0.49	…	0.02	0.02	Bal
EM WM	0.09	0.47	1.62	0.01	0.02	0.24	0.23	1.77	0.02	0.11	Bal
OM WM	0.11	0.42	1.48	0.01	0.01	0.65	0.35	1.97	0.02	0.02	Bal

Note: BM, base metal; UM WM, under match weld metal; EM WM, equal match weld metal; OM WM, over match weld metal

Table 2 Mechanical properties of base metal and WMs

				VHN (30 kg)		Charpy impact energy at RT, J		
Joint	**YS, MPa**	**UTS, MPa**	**Elongation, %**	**WM**	**HAZ**	**WM**	**HAZ**	**MMR**
BM	700	790	19.0	250	…	90	…	…
UM WM	560	660	16.5	230	248	80	74	0.8
EM WM	710	800	15.6	265	280	95	83	1.0
OM WM	810	890	14.8	280	305	110	98	1.16

Note: BM, base metal; UM WM, under match weld metal; EM WM, equal match weld metal; OM WM, over match weld metal; UTS, ultimate tensile strength; VHN, Vickers hardness number; YS, yield strength

Table 3 Welding conditions and process parameters

Welding machine	**DC generator**
Electrode diameter, mm	4.0
Voltage, V	24
Current, amps	160
Welding speed, mm/min	130
Heat input, kJ/mm	1.3
Preheat temperature, °C	150
Interpass temperature, °C	250
Root run	2.5 mm diam electrode

Table 4 Crack growth parameters

Joint type	***m***	***C***	**ΔK_{th}, MPa$\sqrt{m}$**	**ΔK_{cr}, MPa$\sqrt{m}$**	**$\Delta\sigma_e$, MPa**
UM WM	4.20	7.33×10^{-10}	5.5	25	60
EM WM	3.85	1.04×10^{-9}	6.0	35	65
OM WM	3.40	1.59×10^{-9}	6.5	45	70
UM HAZ	4.80	3.25×10^{-10}	5.0	25	50
EM HAZ	4.30	7.15×10^{-10}	5.5	30	55
OM HAZ	3.70	1.75×10^{-9}	6.0	40	60

Note: UM WM, under match weld metal; EM WM, equal match weld metal; OM WM, over match weld metal; UM HAZ, under match heat affected zone; EM HAZ, equal match heat affected zone; OM HAZ, over match heat affected zone

compared with the equally matched (EM) and UM WMs and the HAZ. In other words, the fatigue crack growth rate is much faster in the UM WM and UM HAZ regions when compared with the EM and OM WMs and HAZ regions. This behavior can be inferred from the steeper slope of the crack growth rate curves. This is also observed from the *S-N* curves (Fig. 4). The endurance stress range ($\Delta\sigma_e$) is higher for the OM WMs and OM HAZ region compared with UM and EM joints.

Figure 5 depicts the relationship between the MMR and the ΔK_{th} and the ΔK_{cr}. From Fig. 5, it is understood that ΔK_{th} and ΔK_{cr} are directly proportional to the MMR, if the notch is made in either the weld region or HAZ. Figure 6 reveals the relationship between the MMR and *m*. From Fig. 5, it can be seen that *m* is inversely proportional to MMR, irrespective of notch location.

The better fatigue performance of the OM WM and OM HAZ in any of these regions may be due to any one of the following: (a) superior mechanical properties, (b) ideal microstructure, or (c) favorable residual stress pattern.

4.1 Mechanical Properties

The fracture resistance of a material is mainly influenced by the size of the plastic zone ahead of the crack tip. If the plastic zone is large, the triaxial state of stress at the crack tip is reduced, and the fracture resistance of the material is very high. For a shallow cracked specimen, the plastic zone can easily spread ahead of the crack tip and into the adjacent area. Therefore, a large plastic zone increases the fracture resistance of the material. In a deeply notched specimen, the plastic zone is small, and, hence, stress relaxation becomes difficult and fracture resistance decreases (Ref 15).

In the UM WM, since deformation and yielding are mainly concentrated in the WM zone, extension of the plastic zone lies within the WM. As soon as the plastic zone reaches the fusion line, deformation continues along the interface between the parent material and the WM (Ref 16). The triaxial state of stress is high in the WM, and the relaxation of this stress is poor. The driving force for crack extension is small, and the fracture toughness of the UM metal is not high.

In the OM WM, the plastic zone can easily extend into the lower-strength base alloy because deformation and yielding occur in both the WM and the base alloy. In this case, stress

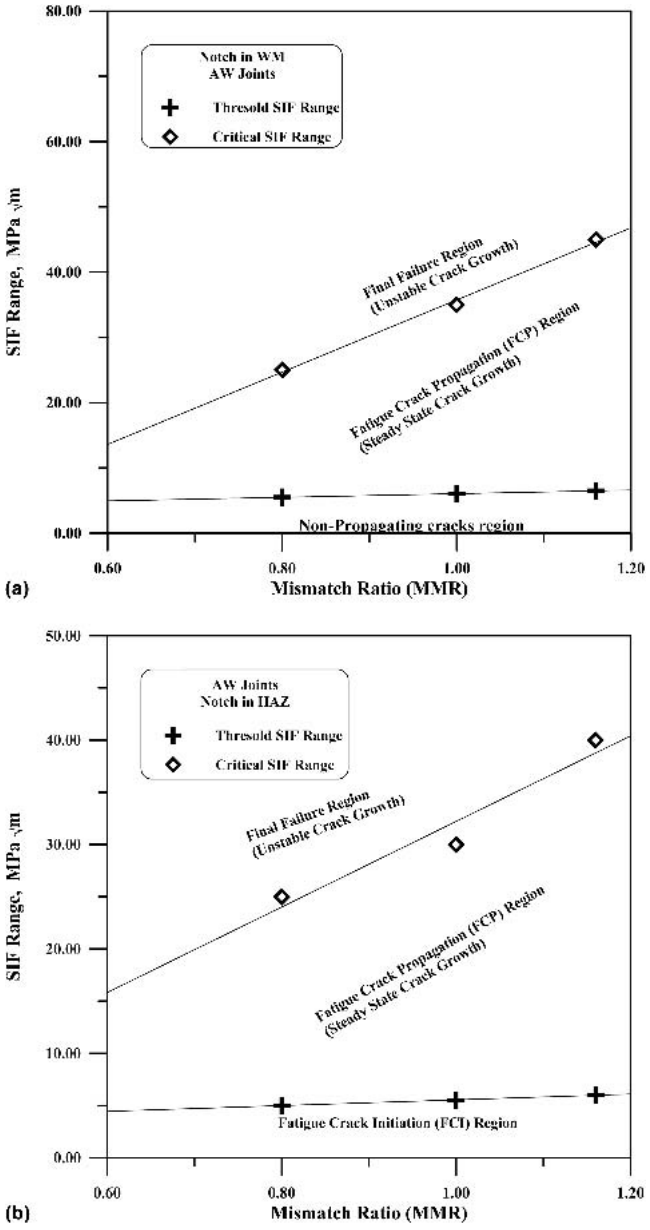

Fig. 5 Relationship between MMR and ΔK_{th} and ΔK_{cr}

relaxation can easily take place in the crack tip region. As a result, a higher crack driving force is needed for crack extension, and the fracture resistance of the OM WM is higher than that of the UM WM (Ref 17). Moreover, Bannister (Ref 18) reported that the OM WM absorbs more energy, leading to an increased Charpy transition temperature for weld center line notched and fusion line notched specimens. This is due to the high alloy content of the WM.

The mechanical properties (i.e., yield strength, tensile strength, and toughness) of the OM WM and the HAZ are superior compared with the EM and UM WMs (Table 3). The higher yield strength and tensile strength of the OM WM is used to enhance the endurance limit of the OM joints, and, hence, fatigue crack initiation is delayed. The higher toughness of the OM WM and the HAZ imparts greater resistance to

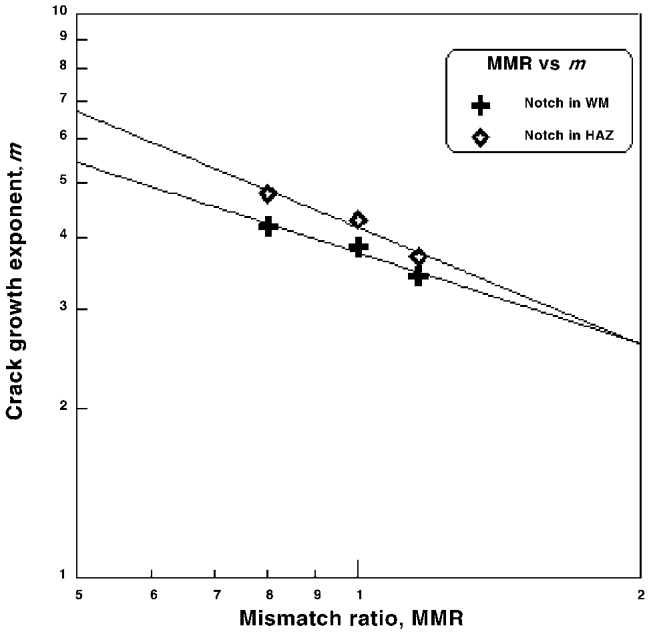

Fig. 6 Relationship between MMR and *m*

fatigue crack propagation, and, thus, the fatigue crack growth rate is comparatively slow. The combined effect of higher yield strength and higher toughness of the OM WM and the HAZ enhances resistance to crack initiation and crack propagation. Therefore, the fatigue performance of the OM WM and the HAZ is superior compared with the EM and UM WMs.

4.2 Microstructure

In the CCT specimen, the notch is machined in the WM region and the HAZ region by wire EDM, so that the crack growth behavior of the WM and HAZ regions can be evaluated under fatigue loading. The crack initiates from the tip of the machined notch and grows into the WM (or the HAZ) until final failure takes place. Thus, the WM and HAZ microstructures will have an influence on the fatigue performance of the joints. Optical micrographs of the WM are shown in Fig. 7. From the micrographs, it can be observed that the WM mainly consists of acicular ferrite (AF), proeutectoid ferrite (PF), and side plate ferrite (SPF). The amount of AF varies in each WM; i.e., OM WM consists of a higher amount of AF, and UM WM consists of lower amount of AF.

As described by Liv and Olson (Ref 19), AF is formed intragranularly, resulting in randomly oriented short ferrite needles with a basket-weave appearance. This interlocking nature, together with its fine grain size, provides the maximum resistance to crack propagation by cleavage. However, the formation of grain boundary ferrite, SPF, or upper bainite is detrimental to WM toughness, since these microstructures provide easy crack propagation paths (Ref 20). From other research (Ref 21-23), it appears that cracks in ferritic WM normally propagate along PF, a process that is intensified by the presence of brittle pearlitic structures along the grain boundaries. This is also evident from the WM mechanical properties. Due

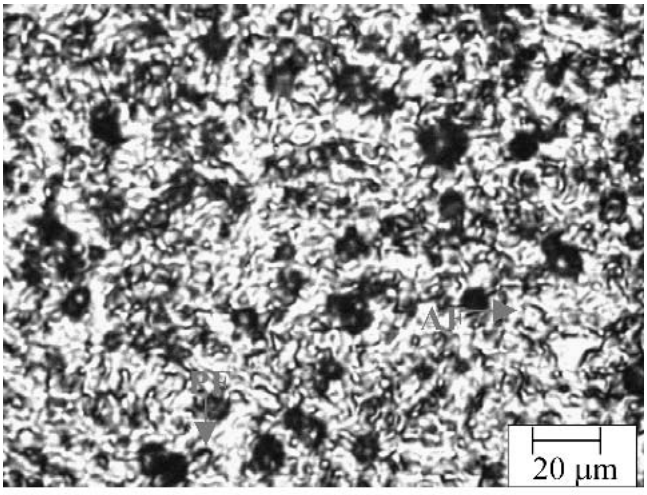

(a)

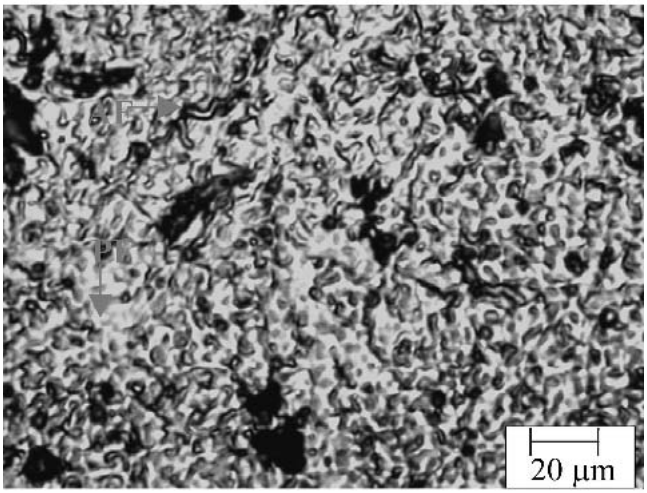

(b)

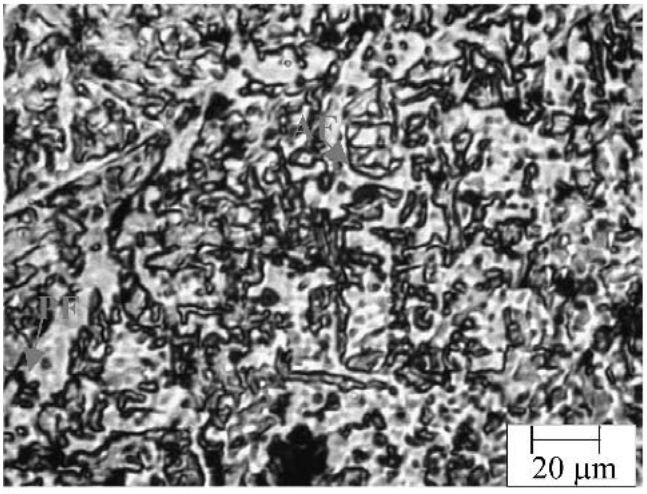

(c)

Fig. 7 Optical micrograph of WMs

to the higher amount of AF present in the OM WM, its toughness is higher than the other WMs and, subsequently, enhances its fatigue performance.

An optical micrograph of the HAZ is displayed in Fig. 8. The HAZ invariably consists of coarse-grained (CG) ferrite in all joints (UM and OM), but the grain size is relatively small in the OM joints compared with the UM joints. It has been reported (Ref 24) that in a single-pass weld the CG HAZ microstructure possesses the lowest toughness. In multipass welding, the microstructure of the HAZ is more complex due to its partial refinement by subsequent passes. In this case, the intercritical (IC) HAZ is responsible for the reduction in toughness. Kocak et al. (Ref 25) have found that the crack tip opening displacement (CTOD) and Charpy impact toughness of CG HAZ depend both on the microstructural features of the CG HAZ and the yield strength of the adjacent WM. Minami et al. (Ref 26) reported that CG HAZ is responsible for brittle fracture initiation in almost all of the samples tested by CTOD. Rajanna et al. (Ref 27) found that the fine-grained structure yielded higher dynamic fracture toughness values than the CG structure.

Spies et al. (Ref 28) reported that the CG structure has a higher threshold level during the early stage of fatigue crack growth, and, hence, the HAZ has higher threshold levels than the base metal. The crack growth rate in the HAZ is found to be slightly higher than that in the base metal. However, in this investigation the early stage of fatigue crack growth was not considered since the minimum crack growth rate observed during the experiments was 1×10^{-6} mm/cycle, which is well above the early stage of fatigue crack growth. Generally, smaller grains will offer better resistance to fatigue crack propagation compared with coarse grains due to the presence of numerous grain boundaries. These grain boundaries act as obstacles for the growing crack (Ref 29). As a result, the fatigue performance of the UM HAZ is inferior compared with that of the OM HAZ.

4.3 Residual Stresses

Residual stresses, arising in welded joints as a consequence of incompatible thermal strains caused by heating and cooling cycles, also have a significant effect on the fatigue life of welded structures (Ref 30). When a fatigue crack is propagating through a residual stress field in a welded plate, the stress intensity at the crack front is influenced by the combined effect of the local residual stress and the stress from the externally applied load. This means that the effective SIF of the crack front is the sum of the SIFs from the residual stress and external loads (Ref 31).

During heating and cooling, the expansion and contraction of the WM is resisted by the surrounding base metal. Due to the restraint offered by the base metal during the expansion and contraction of the WM, a tensile residual stress field is generated in the WM (Ref 32). If the yield strength of the base metal is higher than that of the WM, then the restraint offered by the base metal will be higher and the magnitude of tensile residual stress will be greater. In the UM WM, the tensile residual stress is higher than in the OM WM.

Table 5 shows the measured x-ray residual stress values for two different conditions: as-welded joints (i.e., immediately after welding, the residual stresses are measured in the weld region and HAZ); and as-ground specimens (i.e., at the crack tip of the CCT specimens). In the CCT specimens, the mea-

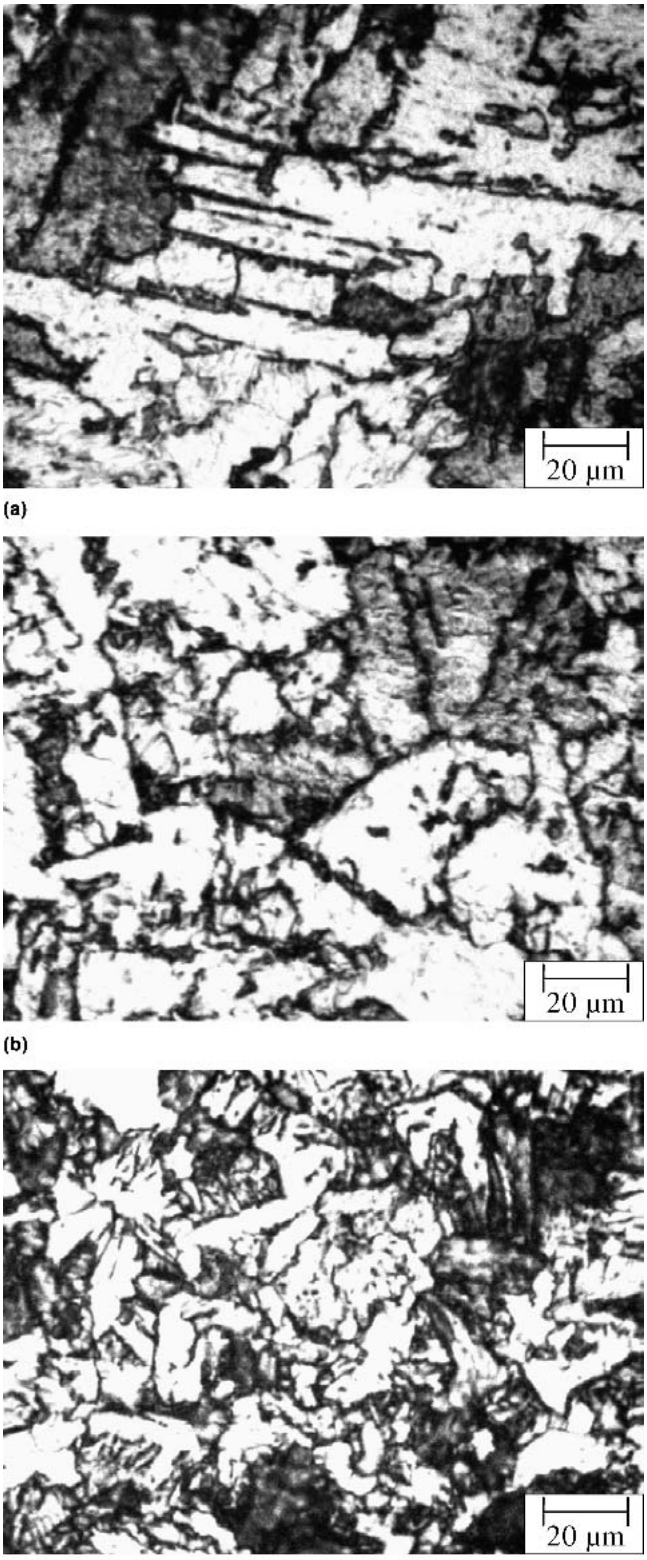

Fig. 8 Optical micrograph of HAZ regions

sured residual stress is compressive and is due mainly to the fact that after welding the joints were sliced, machined, and ground to obtain the required dimensions of CCT specimen.

Table 5 Measured residual stress values

Joint type	Magnitude of residual stress, MPa			
	Welded joint		CCT specimen	
	WM	HAZ	WM	HAZ
UM	+162	+148	−64	−70
EM	+115	+90	−112	−124
OM	+74	+65	−158	−165

Note: UM, under match; EM, equal match; OM, over match

Due to the aforementioned sample preparation operations, the original tensile residual stresses caused by the welding operation were relieved. Subsequently, compressive stress fields were generated due to the compressive load acting on the specimen during grinding. Even though the compressive load is the same for all specimens (i.e., UM, EM, and OM), the resultant residual stresses are different due to residual stress differences in the original as-welded samples. From the measured residual stress values (Table 5), it can be inferred that the magnitude of the compressive stress field in the OM weld region and the HAZ is higher than that in the EM and UM joints. This may be the reason for the slower fatigue crack growth rate observed in OM joints since compressive residual stresses usually retard the rate of fatigue crack growth (Ref 33, 34).

5. Conclusions

The present investigation has been carried out to study the effect of notch location on fatigue crack growth behavior and fatigue life in shielded metal arc welded, strength-mismatched HSLA steel welds. From this investigation, the following conclusions have been obtained:

- The fatigue crack growth behavior and fatigue life of the welded joints are influenced by notch location and MMR. In summary, the fatigue crack growth behavior and fatigue performance are superior when the notch is machined in the WM, irrespective of the MMR.
- The MMR is inversely proportional to the fatigue crack growth exponent (m) and is directly proportional to the threshold SIF (ΔK_{th}) and the critical SIF (ΔK_{cr}), irrespective of notch location.
- OM joints offer greater resistance to fatigue crack growth, and, hence, the fatigue performance of the OM joint is superior to the EM and UM joints, regardless of notch location.

Acknowledgments

The first two authors are grateful to Prof. S. Nemat Nasser, Director of the Center of Excellence for Advanced Materials, University of California at San Diego, USA, for providing financial and infrastructural facilities in performing the fatigue crack growth experiments during the recent visit of Dr. Balasubramanian to UCSD. The authors also wish to thank Department of Manufacturing Engineering, Annamalai University for supporting this investigation.

References

1. R. Denys, "Provisional Definitive Statement on the Significance of Over and Under Matching Weld Metal Strength," IIW Doc. X-1222-91, International Institute of Welding, 1991
2. K. Angamuthu, B. Guha, and D.R.G. Achar, Investigation of Dynamic Fracture Toughness Behaviour of Strength Mis-Matched Q & T Steel Weldments Using Instrumented Charpy Impact Testing, *Eng. Fracture Mech.,* Vol 64, 1999, p 417-432
3. T. Matsumoto, F. Suzuki, Y. Wadayama, H. Sato, and M. Tsukamoto, Undermatched Joints in Superconducting Coil Cases of Fusion Reactors, *Welding Int.,* Vol 6 (No. 9), 1992, p 700-706
4. V.G. Nosov and S.M. Shur, Evaluating Effects of Mechanical Heterogeneity on Brittle Strength of Glad-Metal Joints, *Sov. Energy Technol.,* Vol 9, 1986, p 19-21
5. W. Burget and D. Memhard, "Weld Metal Yield Strength Mismatch Effects in Fracture Toughness Test Specimens," IIW Doc. X-F-011-94, International Institute of Welding, 1994
6. Y.J. Kim, "Strength Mis-Match Effect on Local Stresses and Its Implication to Structural Assessments," IIW Doc. Sc.X-F-081-98, International Institute of Welding, 1998
7. I. Rak and A. Treibar, "Weld Joint Fracture Behaviour of HSLA Steels Dissimilar in Strength," IIW Doc X-F-062-97, International Institute of Welding, 1997
8. G.X. Cheng, Z.B. Kuang, Z.W. Lou, and H. Li, Low Cycle Hysteresis Energy for Welded Joint With Mechanical Heterogeneity, *Acta Metall.,* Vol 29 (No. 7), 1993, p A328-A333
9. G. Cheng, Z.B. Kuang, Z.W. Lou, and H. Li, Experimental Investigation of Fatigue Behaviour for Welded Joint With Mechanical Heterogeneity, *Int. J. Pressure Vessels Piping,* Vol 67, 1996, p 229-242
10. J. Onoro and C. Ranninger, Fatigue Behaviour of Laser Welds of High Strength Low Alloy Steels, *J. Mater. Proc. Technol.,* Vol 68, 1997, p 68-70
11. P.C. Paris and F.A. Erdogan, A Critical Analysis of Crack Propagation Laws, *Transac. ASME J. Basic Engineering,* Vol 85, 1963, p 528-534
12. G.E. Dieter, *Mechanical Metallurgy,* McGraw Hill, 1989, p 352
13. M. Isida, On the Determination of Stress Intensity Factors for Some Common Structural Problems, *Eng. Fract. Mech.,* Vol 2, 1970, p 61-79
14. A. Hobbacher, "Recommendations for Fatigue Design of Welded Joints and Components," IIW Doc., No. XIII-1539-96/XV-845-96, International Institute of Welding, 1996
15. W. Tang and Y.W. Shi, Influence of Strength Matching and Crack Depth on the Fracture Parameters of Welded Joints, *Proceedings of ESIS 17 on Mis-Matching of Welds,* Mechanical Engineering Publications, London, 1994, p 433-443
16. C. Eripret and P. Hornet, Prediction of Overmatching Effects on the Fracture of Stainless Steel Cracked Welds, *Proceedings of ESIS 17 on Mis-Matching of Welds,* Mechanical Engineering Publications, 1994, p 685-708
17. G. Lin, X. Meng, A. Cornec, and K.H. Schwalbe, "Numerical Study of the Effect of Strength Mis-Match on the Crack Growth Behaviour," IIW Doc. Sc. X-F-063-97, International Institute of Welding, 1997
18. P. Bannister, Fracture Behaviour of Mis-Matched Welded Joints in a Quenched and Tempered Steel of 800 MPa Yield Stress, *Mismatching of Interfaces and Welds,* GKSS Research Centre Publications, 1997, p 599-612
19. S. Liv and D.L. Olson, The Role of Inclusions in Controlling HSLA Steel Welds Microstructures, *Welding J.,* Vol 65, 1986, p 139s-149s
20. R.A. Farrar and Z. Zhang, Aspect Ratios and Morphology of Acicular Ferrite in C-Mn-Ni Weld Metals, *Mater. Sci. Technol.,* Vol 117, 1995, p 759-764
21. E. Levine and D.C. Hill, Toughness in HSLA Steel Weldments, *Metal Construct.,* Vol 9, 1977, p 346-353
22. J. Dixon and K. Hakansson, Effect of Welding Parameters on Weld Zone Toughness and Hardness in 690 MPa Steel, *Welding J.,* Vol 74, 1995, p 122s-132s
23. V. Balasubramanian and B. Guha, Effect of Welding Processes on Fatigue Crack Growth Behaviour of ASTM 517 "F" Grade Steel Weldments, *Sci. Technol. Welding Joining,* Vol 4, 1999, p 265-276
24. J. Healy, J.P. Billingham, J.P. Chubb, R. Jones, and J. Galsworth, The Influence of Relative Weld Metal/Parent Plate Yield Strength on the Resultant Fracture Path in Impact Testing Of Very High Strength Welded Steels, *Proceedings of ESIS 17 on Mis-Matching of Welds,* Mechanical Engineering Publications, 1994, p 789-795
25. M. Kocak, M. Es-Souni, L. Chen, and K.H. Schwalbe, Microstructure and Weld Metal Matching Effects on Heat Affected Zone Toughness, *Proceedings of the 8th International Conference on Offshore Mechanics and Arctic Engineering,* The Hague, Netherlands, 1989, p 623-630
26. F. Minami, M. Ohta, and M. Toyoda, Prediction of Specimen Geometry Effect on Fracture Resistance of HAZ Notched Welds by Local Approach, *Mismatching of Interfaces and Welds,* Schwalbe and Kocak, Ed., GKSS Research Centre Publications, 1997, p 319-325
27. K. Rajanna, S.K. Bhambri, and D.R.G. Achar, An Assessment of a CrMoV Cast Steel Weld Joint for Dynamic Fracture Behaviour, *Eng. Fract. Mech.,* Vol 29 (No. 4), 1988, p 387-399
28. H.J. Spies, C. Pusch, C. Henkel, and K. Robler, Fatigue Crack Propagation in High Strength Low Alloy Steels, *Theory Appl. Fract. Mech.,* Vol 11, 1989, p 121-125
29. J.P. Benson, Influence of Grain Size and Yield Strength on Threshold Fatigue Behaviour of Low Alloy Steel, *Mater. Sci.,* Vol 9, 1979, p 535-539
30. S.J. Maddox, *Fatigue Strength of Welded Structures,* Cambridge University Press, 1991
31. W. Elber, *Fracture Toughness and Slow Stable Cracking,* STP 559, ASTM, 1974, p 45
32. R.S. Parmar, *Welding Engineering and Technology,* Khanna Publishers, 1999
33. T.N. Nguyen and M.A. Wahab, The Effect of Residual Stresses and Welds Geometry on the Improvement of Fatigue Life, *J. Mater. Processing Technol.,* Vol 48, 1995, p 581-590
34. D. Radaj, *Design and Analysis of Fatigue Resistance of Welded Structures,* Abington Publishing, 1990